Thermal energy storage with phase change materials in solar power plants. Economic analysis

Cristina Prieto [a,b], Luisa F. Cabeza [c,*]

[a] *Abengoa, Department of Solar Technology, Energía Solar 1, 41014 Sevilla, Spain*
[b] *University of Seville, Department of Energy Engineering, Camino de Los Descubrimientos S/n, 41092, Seville, Spain*
[c] *GREiA Research Group, Universitat de Lleida, Pere de Cabrera s/n, 25001 Lleida, Spain*

A B S T R A C T

Thermal energy storage (TES) increases concentrating solar power (CSP) plant capacity factors, but more important, improves dispatchability; therefore, reducing the capital cost of TES systems is very important to reduce cost of energy and serve as an enabler for commercial solar power plants. After presenting the concept of a novel cascade PCM configuration of CSP and demonstrating it energy efficiency, it is needed to develop a thoughtful economic evaluation of the concept. The goal of this paper was to investigate this system through annual modelling, engineering procurement company price quotes, and levelized cost metric comparison with a baseline case, the commercial two-tank molten salt storage system. Simulation results show that this new PCM concept decrease levelized costs of storage. The baseline of using shell and tube heat exchangers for PCM storage offers a reduction in capital and levelized cost, but this paper also shows that there are further cost reduction possibilities, as shown in the scenarios presented here, such as thermal conductivity enhancement, encapsulation of the PCM, or modification of the material to improve its thermal properties. Therefore, although the basic shell and tube PCM system has been shown to offer a cost savings, the 1.8% reduction in LCOE may not be worth the risk of further development. The shell and tube system should be a jumping off point to more appropriate technologies. The variants studied are likely to yield cost reductions in cost performance quotient (CPQ) as high at 80% and in LCOE as high as 10%, representing an unprecedented and valuable avenue of CSP plant cost reduction.

1. Introduction

Commercial concentrated solar power (CSP) is more accommodating to energy storage than other solar technologies. Energy can be stored at relatively high efficiencies in the form of thermal energy. Thermal energy storage (TES) increases plant capacity factors and improves dispatchability. Reducing the capital cost of TES technologies will also result in a reduced cost of energy and ultimately serve as an enabler for commercial solar power plants [1]. The development of reliable, flexible and cost-efficient molten salt storage system has recently been acknowledged by the CSP community as a potential major enabler of a better integration of CSP with other cheap variable renewables, by potentially facilitating smart control of co-located assets through smoothening the fast variations from PV and/or wind. The integration of TES systems into large-scale CSP plants is a cost-effective way to reduce the Levelized Cost of Electricity (LCOE) in a solar plant [2–4], being the

binary mixture of sodium and potassium nitrate the most used storage medium [5]. Several studies are looking for a way to reduce the cost of TES through the use of new storage material [2,3,6] and several reviews have been published with different TES technologies under development [7]. One of the development most analysed are PCMs due to their higher energy density [8]. Presently, many PCM sizing models were generated to model both PCM TES systems [9–11]. These models focus on calculating a cost per kWh of thermal energy storage. This is accomplished in one of two ways: a performance efficiency is assumed and the size is calculated directly [5,12] or a performance efficiency is calculated based on assumptions and the size is calculated [9–11]. While the latter method is considerably more accurate, it still relies on a generalization of the TES performance over the course of a whole year. This modelling method is suspect due to the inability of simple performance models to capture the realistic response of passive TES systems to transient energy flows observed in a CSP plant. This intrinsic modelling difficulty was
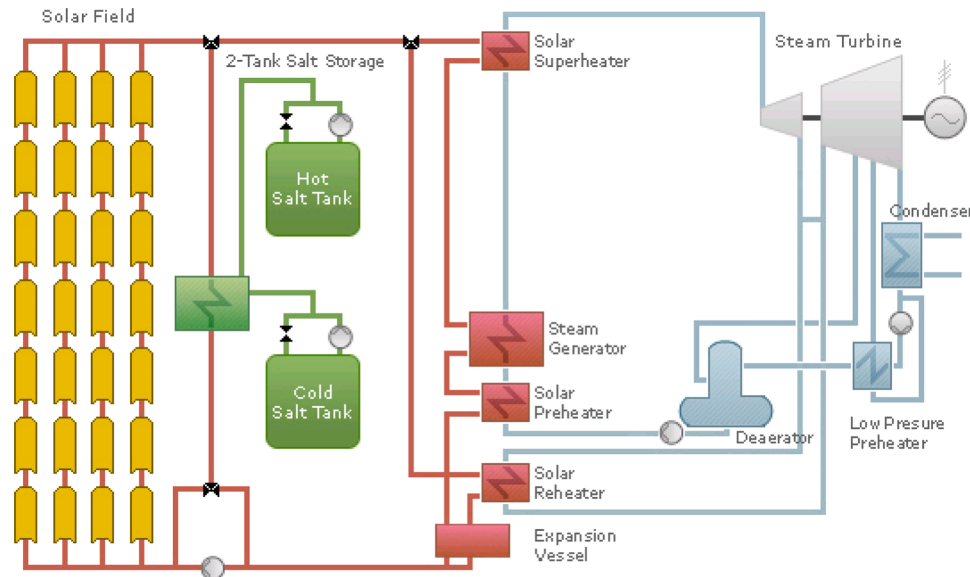
Fig. 1. Baseline plant configuration with indirect two-tank molten salt TES [17].

Table 1
Baseline CSP plant and TES specifications.

Component	Baseline
General	
Plant Location	Phoenix, AZ
Turbine Name Plate Capacity (gross)	144 MWe_gross
Plant Name Plate Capacity (net)	125 MWe_net
Solar Multiple	2.0
Power Block	
Power Cycle	Superheated steam Rankine cycle with reheat
Feed-water Heaters	5
Steam Inlet Pressure	100 bar (absolute)
Condenser Pressure	0.08 bar (absolute)
Steam Inlet/Reheat Temperature:	373.0/373.0 °C
Feed-water Temperature:	234 °C
Cooling	Wet
Solar Field	
Field Style	Parabolic Trough
Field Layout	"H" configuration
# of Loops	428
Module Aperture	5.76 m
Solar Field HTF	Therminol VP-1
Field Supply Temperature	393 °C (nominal)
Field Return Temperature	293 °C (nominal)
Thermal Energy Storage	
Storage Type	Indirect 2-tank molten salt
Storage Capacity	6 equivalent full load hours (864 MWh_e_gross)
Number of Tanks	3 hot/3 cold
Storage Fluid	Binary salt (60% $NaNO_3$, 40%KNO_3)
Storage Fluid Quantity	66,613 metric tons
Hot Tank Temperature	386 °C
Cold Tank Temperature	295 °C

overcome in some cases with experimental work. These experiments reinforced the low capitol cost potential of PCM TES systems. However, they still lack a realistic look at the response of passive TES systems to transient energy flows anticipated in CSP plants.

Zhao et al. [13] studied the influence of different key design parameters on the performance of a packed bed PCM system for a CSP tower plant. Those authors withdraw interesting conclusions on the effect of the design parameters of the packed bed PCM tank in the costs of the storage plant, such as the dimensions of the storage tank or the needed volume of PCM to shorter operation duration while not increasing too much the capital costs.

Caceres et al. [14] calculated the levelized cost of energy when suing

copper foams in PCM tanks, to reduce the storage volume and increase the thermal conductivity of the storage material. This economic analysis showed that using copper foams in PCM storage systems can reduce the required storage volume by 77%, however the cost of the copper foam significantly increases the total cost of the plant.

Also considering the low thermal conductivity of PCM storage systems, Jacob et al. [15] compared environmentally and economically two storage system in CSP plants: a packed be PCM system and a liquid metal-based TES system. In that study, only the capital expenditure (CAPEX) was calculated, finding that the PCM system had a lower CAPEX than previous studies about encapsulated PCM systems that could be found in the literature. Those authors already highlighted that the CAPEX of the PCM system would benefit from further optimisation with new concepts such as the cascade PCM systems.

But there is not a thoughtful economic evaluation of a PCM storage plant for CSP. Moreover, the cascade PCM concept was shown as energetically effective in the first part of this study [16]. The goal of this paper was to investigate this system through annual modelling, engineering procurement company price quotes, and levelized cost metric comparison with a baseline case, the commercial two-tank molten salt storage system.

2. System description

2.1. Baseline TES system

The selected baseline system for comparison was the commercial state-of-the-art indirect two-tank molten salt TES technology. Fig. 1 shows the configuration of a SP plant with this TES system. Table 1 presents the specifications of the system. This study considered a TES capacity of 6 equivalent full load hours (EFLH) of indirect storage since this is representative of systems currently commercially considered. All calculations assume the plant is located near Phoenix, AZ (United States). The considered size of the plant is 144 MW_e_gross.

2.2. PCM cascade configuration for simulation

The PCM system evaluated at simulation scale is based on a cascade concept, where storage tanks containing PCM with different melting temperatures are connected in series (Fig. 3). The heat transfer fluid (HTF) runs through a heat exchanger where its energy is charged and discharged. A detailed description of the PCM cascade storage system
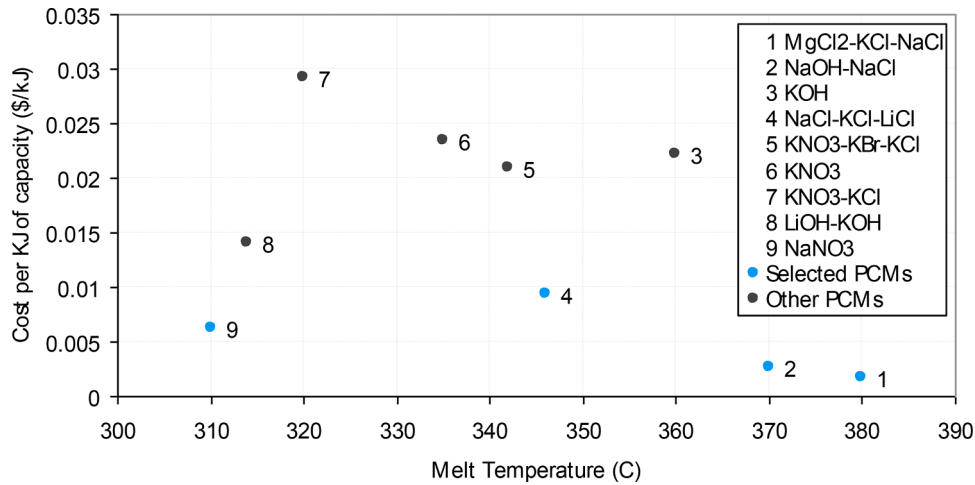
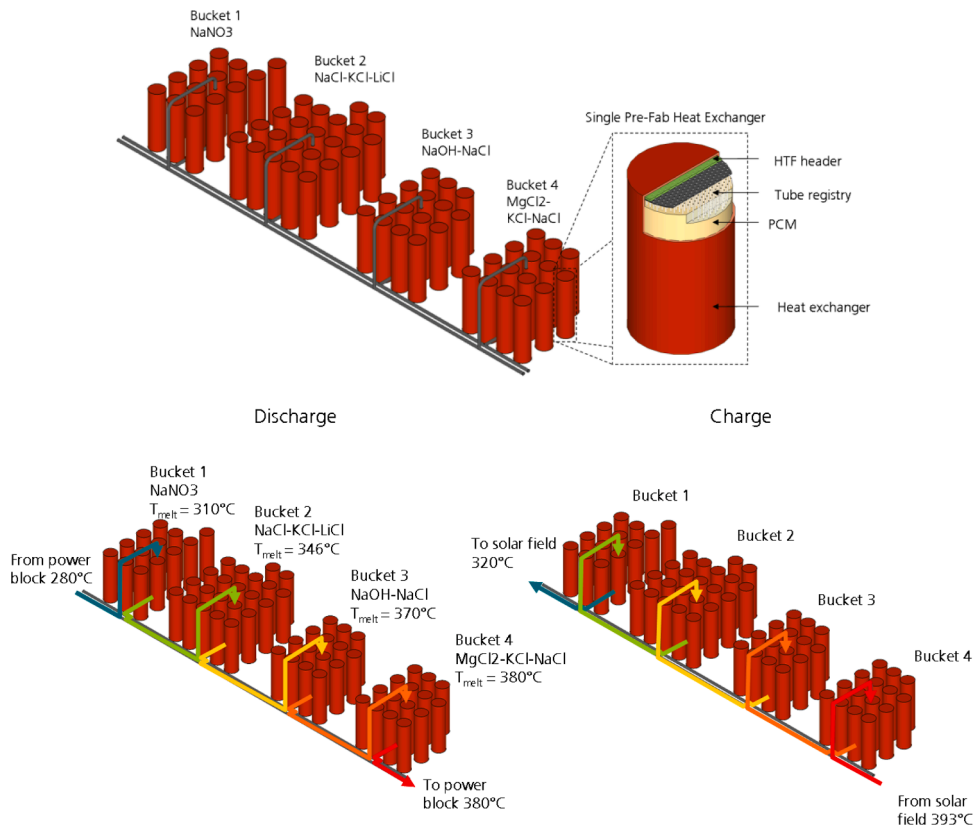**Fig. 2.** Cost per kJ of each PCM considered [16].

Fig. 3. Depiction of the entire PCM cascade and a single pre-fabricated heat exchanger [16].

evaluated in this paper and its energetic performance is developed in a previous paper [16]. Phase change materials were selected from those available in the literature [18] based on its cost per capacity (Fig. 2)

There are possible scenarios that attempt to mitigate some of the problems inherent in the basic PCM TES system. These variations attempt to ameliorate the thermal issues of PCM storage by altering the physical layout of the PCM system or the constituent materials of the system. Current variations under consideration are: thermal conductivity enhancement, use of the optimal melting temperature PCM, use of the ideal properties of the PCM, PCM encapsulation, enhanced ideal properties, and compact heat exchanger utilization, and will be detailed later on.

2.3. Concept specifications

The considered plant was a 6 h storage system for a 125 MW net parabolic trough plant using Therminol VP1® as heat transfer fluid (HTF). This storage system represents six hours of full load output in a representative day: May 25th using Phoenix Arizona TMY2 data.

There are many configurations of PCM systems that would work for the above storage performance specification of 6 h at full load. Because the simulation of the PCM system is an inherently more complex system then the two tanks baseline, there are more parameters that can be altered to adjust the performance. These parameters are summarized in Table 2.

One major benefit of the PCM TES concept is its reduction of

Table 2
Design parameters used in the model PCM model.

Parameter	Description	Range or typical value
Number of PCMs	Number of phase change materials in the cascade	1-10
PCM type	Chemical formula of PCM in each bucket (sets thermal properties)	All known substances
Tube length	Tube length for each bucket	100 - 1000 (m)
Number of tubes	Number of tubes in each bucket	100 - 10,000
Extent radius	Extent radius of PCM around the tube for each bucket	1.5-20 (cm)
Tube outer diameter	Outer diameter of heat exchanger tube set by EPC	0.0254 (m)
Tube inner diameter	Inner diameter of tube set by EPC	0.022 (m)
Alpha	Void fraction of any heat transfer enhancement	0-100%
Ideal melting point	Ideal melting point of salt if melting point manipulation is being used	±25
Percent power block reroute	The percent of the power block mass flow that is first routed through the hottest bucket	0-100%
Heat exchanger material	Material being used to build the heat exchanger (sets thermal properties)	Stainless steel

Table 3
Technical description of heat exchangers used in the system.

Type	Single pass shell and tube
Diameter	4.3 (m)
Length	19.8 (m)
Count	64
Material	310 or 304 stainless steel
Configurations	HTF flows in tube side while PCM is stored on shell side. Heat exchangers are arranged into groups in series and parallel to achieve correct effective tube length and numbers.

Table 4
Technical description of materials used in the system [18].

Variable	Bucket 1	Bucket 2	Bucket 3	Bucket 4
Chemical (mass %)	$NaNO_3$	NaCl (33%) KCl (24%) LiCl (43%)	NaOH (80%) NaCl (20%)	$MgCl_2$ (60%) KCl (20.4%) NaCl (19.6%)
Melting point (°C)	310	346	370	380
Enthalpy of fusion (kJ/kg)	172	280	370	400
Thermal conductivity liquid (W/m-K)	0.56	0.68	0.87	1.08
Thermal conductivity solid (W/m-K)	0.56	2.65	2.35	2.29
Solid density (kg/m³)	1929	1897	2104	2055
Liquid density (kg/m³)	1882	1512	1743	1609
Specific heat (kJ/kg•K)	1.82	1.34	2.01	1.04
Kinematic viscosity (m²/2)	1.51E-06	7.94E-07	1.92E-06	9.63E-07
Volumetric expansion (%)	2.5%	25.5%	20.7%	27.7%
Mass in system (kg)	3,122,644	7,292,907	6,527,257	3,747,172

Table 5
Financial and incentive assumptions from CSP FOA with modifications.

Financial assumptions	Value	Comments
Analysis period	30 years	—
Inflation rate	2.5 %	—
Real discount rate	8.0 %	—
Federal tax	34%/year	National Energy Technology Laboratory (NETL) 2007
State tax	6%/year	NETL 2007
Property tax	0	—
Sales tax	7.75%	—
Insurance	0.50%	—
Loan term	20 years	—
Loan rate	8.00 %	—
Loan (Debt) fraction	50.0%	NETL 2007
Federal depreciation rate	—	MACRS Mid-Quarter Convention for solar
State depreciation rate	—	MACRS Mid-Quarter Convention for solar
PPA escalation rate	1%	—
Minimum required IRR	12.0%	NETL 2007
Minimum required debt service coverage ratio (DSCR)	1.40	—
Incentives: Federal investment tax credit (ITC)	30%	was 10% in DE-FOA-0000104

Cost assumptions	Value	Comments
Contingency	Included in EPC quote	—
Engineer, procure, construct	Included in EPC quote	SAM default of 16% was used on DE
Project, Land, Misc.	Included in EPC quote	SAM default of 3.5% was used on DE
Percentage of direct costs subject to Sales Taxes	80%	SAM default

heat exchangers, PCM, charge/discharge valve setup and salt melting equipment.

The heat exchangers are the largest cost system component. They not only facilitate the transfer of energy from the HTF to the PCM, but also contain the PCM. The heat exchangers used in this project are based on prefabricated heat exchangers that can be shipped to the site. As such, the diameter and length were constrained to a shippable size. Table 3 gives the technical description of the heat exchangers.

The PCM is broken down by bucket. Initially, all PCMs between the hot and cold design temperatures of the plant were considered. Table 4 gives the technical specifications for the PCMs used in the current system. The table shows the volume expansion of the salts, that is one of the main challenges of the PCM. The PCMs currently being considered undergo a density change of almost 25%, as such, thawing stress can be a serious issue. The heat exchangers oriented in a vertical orientation were proposed as an option to minimize the structural yielding in freeze-thaw cycles. This change eliminates thawing stress because the expanding liquid is given an avenue for escape. The HTF is always fed into the top of the heat exchanger and, as such, the initial PCM melting starts at the interface of the PCM and the gas in the expansion head. As the rest of the PCM melts it can expand out the avenue of previously melted PCM.

Another key piece of equipment is the salt melting setup. When the plant is being constructed, the PCM must be pumped into the tanks in molten form. Although this seems like a trivial task, the mass of PCM required leads to a either a long melting process or a large melting machine [19]. Currently, this machinery has not been fully developed. A cost estimate was obtained, but an economic optimization was not completed. One avenue to higher cost savings over the baseline that was not investigated to date is the removal of the melting system altogether. If the salt can be added to the system in solid form and then melted by the hot HTF instead of a burning fossil fuel, the costs would be probably lower than those considered in this paper.
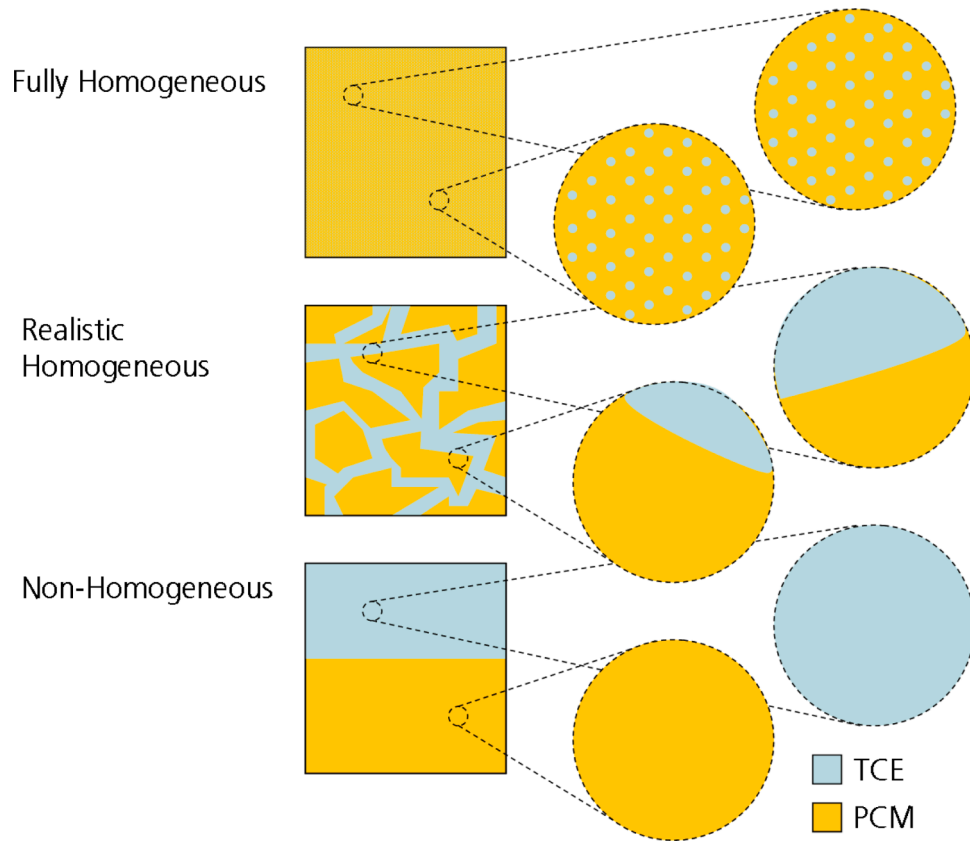
components when compared to the baseline TES system. This is mostly due to the passive nature of the system and removal of the pumping, piping, valves, and elevating structures that are required to operate an active system like the two tanks. The main system components are: the

Fig. 4. Typical representation of fully homogeneous, realistic homogeneous, and non-homogeneous thermal conductivity enhancement techniques.

3. Economic analysis

The physical and performance dissimilarities of the two systems mean that a simple performance-based comparison is not an effective way to determine which system is more fit. As such, an economic analysis was needed in order to generate levelized cost vs. performance metrics like LCOE. This allowed for the two technologies to be compared in a direct way.

The economic analysis was carried out with detailed cost estimates of both systems by an engineering, procurement and construction (EPC) contractor. After several iterations on the cost, final prices were determined for each system.

The Solar Advisor Model (SAM) version 2009.10.13 was used to calculate the levelized cost of energy (LCOE) so that the various concepts can be compared to each other and to the baseline plant. Because SAM is not equipped to analyse the performance of these new storage schemes, the "Generic Fossil, Utility IPP" plant type is used in SAM, which requires the reduction of the TRNSYS performance results to a single annual capacity factor. Financial parameters are taken, in part, from a Department of Energy (DOE) Funding Opportunity Announcement (DE-FOA-0000104) on baseload concentrating solar power generation, which outlined a financial model for use with SAM. Assumptions used in the financial model are summarized in Table 5. The resulting ranges of LCOE are subject to the ±20% EPC cost uncertainty required by accepted estimating practices.

4. Scenarios considered

4.1. Thermal conductivity enhancement (TCE)

When considering thermal conductivity enhancement there is a range of available homogeneity: fully homogeneous, realistic homogeneous, and non-homogeneous. A fully homogeneous system might be

evenly spaced nanoparticles. A realistic homogeneous system might be a large pore metal foam, carbon foam, or loose metal fill. A non-homogeneous system might be fins or large stacked structures. Fig. 4 shows an example of each of these systems on a macro- and micro-scale.

Due to their extreme costs, fully homogeneous systems are outside of the scope of this study. This leaves realistic homogeneous and non-homogeneous systems to be considered. The performance of non-homogeneous systems is not anticipated to be acceptable for our application, therefore, realistic homogeneous systems are considered.

Assuming that the thermal conductivity enhancement will be realistically homogeneous, Eq. (1) can be used to derive the bulk thermal conductivity of an enhanced PCM storage material according to Mesalhy bulk thermal conductivity equation [20]:

$$k_{bulk} = \frac{\left[k_{pcm} + \pi \left(\sqrt{\frac{1-\alpha}{3\pi}} - \frac{1-\alpha}{3\pi} \right)(k_{TCE} - k_{PCM}) \right] \left[k_{PCM} + \frac{1-\alpha}{3}(k_{TCE} - k_{PCM}) \right]}{k_{pcm} + \left[\frac{4}{3} \sqrt{\frac{1-\alpha}{3\pi}}(1-\alpha) + \pi \sqrt{\frac{1-\alpha}{3\pi}} - (1-\alpha) \right](k_{TCE} - k_{PCM})}$$

(1)

This equation was implemented into the PCM TRNSYS component to allow for systems with a new bulk thermal conductivity to be modelled [16]. Additionally, the specific heat and density are also updated based on the thermal conductivity enhancement material being used and the specified void fraction (α).

Once the model was capable of calculating a bulk thermal conductivity, specific heat, and density based on a composite void fraction, it was used to generate a break-even function. A break-even function is a curve showing the amount of money that can be spent on TCE for a range of systems with the same LCOE. To calculate this function, a set of 15 systems were parametrically derived with the same annual capacity factor. The TCE level of each system was modified to meet a target average thermal conductivity improvement for the system. The
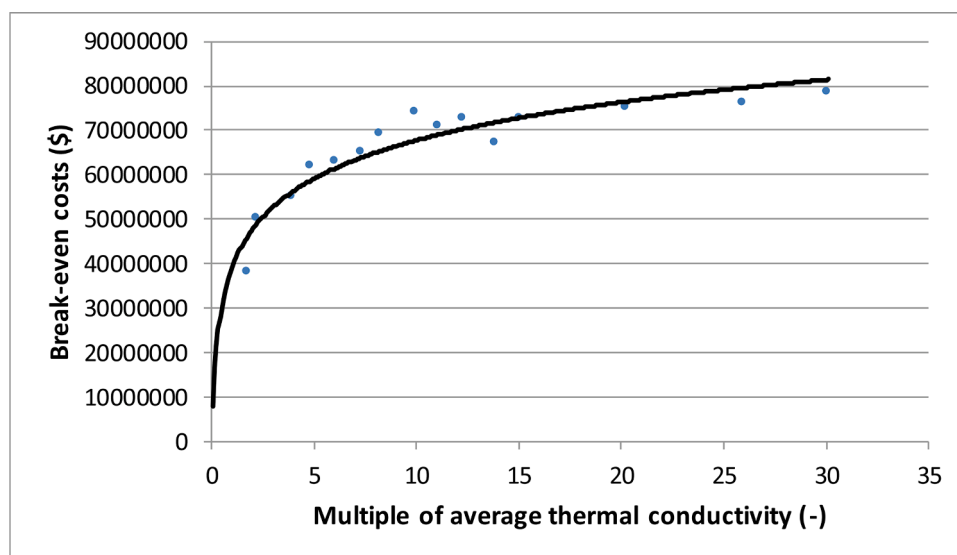
Fig. 5. Break-even cost of the 15 TCE ordered by amount of TCE.

improvement in the average thermal conductivity ranged from 1.4 to 30 times the average thermal conductivity over all the buckets. The break-even function represents TCE costs for each system if it were to perfectly match the LCOE of the basic system (i.e. no real economic improvement). This value is plotted against TCE level in Fig. 5.

The break-even function represents the maximum TCE cost to achieve a lower LCOE. It is also important to note where the cost reduction is occurring in the system. It immediately becomes apparent what level of TCE is most appropriate for a shell and tube based PCM system. Although cost savings go up as TCE level is increased, the trend is one of diminishing returns. This trend exists because there is a shift in the thermodynamic constraint to the resistance on the HTF side as more TCE is added to the PCM.

With no TCE in the system, the heat transfer is constrained by the surface area of the heat exchanger and the thermal conductivity of the PCM. As TCE is added the constraint of the PCM thermal conductivity is alleviated leading to systems with drastically reduced heat exchanger costs. However, around 6-10 times the thermal conductivity of the PCM, this bottleneck is largely minimized. At this level of TCE, the constraint shifts to the internal convection of the HTF. As more TCE is added to the system, the thermal resistance of the HTF convection remains unchanged and the system still requires the same heat exchanger area.

Coupling the diminishing benefit of increasing TCE with cost, it becomes clear that a low level of TCE is optimal. As the level of TCE is increased by decreasing the void fraction, the volume and cost of TCE material increases linearly. Therefore, there is an optimal amount of TCE for any given material based on the break-even cost, the material cost, and the material thermal conductivity.

With the break-even function for our system, it is possible to assess the viability of different TCE materials. The break-even function shows that having the most thermally conductive material possible is not necessarily the best approach. To the contrary, it shows that a material with the appropriate thermal conductivity and a low cost is likely to have a much lower system cost then a high-tech, high thermal conductivity, expensive material.

Before the materials are listed, it is important to note that an in-depth compatibility study has not been performed. Material corrosion in the presence of the materials was kept in mind in the selection but it was not thoroughly researched.

First, metals were considered. Metals tend to have high thermal conductivity and known commodity prices. Furthermore, many metals like steel and aluminium have well developed recycle bound waste streams: available pre-manufactured used materials that are on their

Table 6

Metals considered as thermal conductivity enhancement materials [21].

Metal	Conductivity [W/m•K]	Density [kg/m³]	Price [$/lb]
Silver	410	10295	18.3
Copper	378	8779	7.7
Aluminium	230	2635	2.0
Brass	150	8667	3.0
Tungsten	136	10215	47
Zinc	104	6922	2.2
Cadmium	90	8387	6.6
Platinum	72	21255	39.29
Nickel	66	8772	16
Iron	53	7765	0.104
Lead	31	10992	2.3

Table 7

Non-metallic materials considered.

Material	Conductivity [W/m•K]	Density [kg/m³]	Price [$/kg]	Reference
Silicon carbide	300	3100	2.5	[22]
Graphite fibres	1000	1880	10.0	[23]
Beryllium oxide	106	2979	363.4	[24]
Carbon foam	1950	2210	100.0	[25]

way to be reformed into another product. Since the TCE material is not a load bearing material, the strength and grain purity are not of huge concern and scrap or recycled material represents a perfect source. Table 6 shows a list of metallic materials considered as TCE candidates.

Additionally, non-metallic materials were considered (Table 7). These materials may offer better thermal properties; however, their prices are considerably less commoditized. Furthermore, they will likely involve more processing cost then their metallic counterparts as well defined recycle bound waste streams do not exist.

From this list the break-even function was used to match materials to certain levels of TCE based on the cost and thermal conductivity of the material. Stepping from one level of TCE to the next results in a decrease in system cost. At the same time, this step requires an increase in volume of TCE material and cost. The first step from 1 to 1.4 times the thermal conductivity of the PCM results in large cost savings but does not require
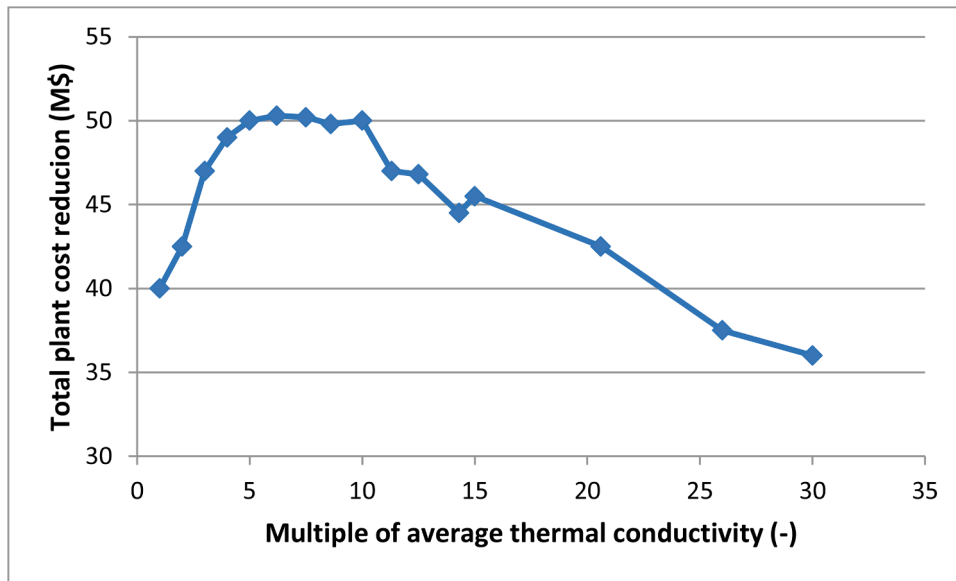
Fig. 6. Plant cost reduction at various levels of thermal conductivity enhancement for aluminium based enhancement.

Table 8

Thermal conductivity enhancement materials that showed promise towards system cost reduction with selected void fraction and cost.

Material		Conductivity multiplier (-)	Foam cost ($)	Void fraction (-)
Aluminium	Raw	7.4	2,368,298	0.919
	Processed	7.4	4,640,591	0.919
Brass	Raw	2.5	4,726,152	0.959
	Processed	2.5	9,452,304	0.959
Iron	Raw	6.2	5,490,521	0.8891
	Processed	6.2	10,981,041	0.8891
Silicon	Raw	8.6	2,619,800	0.977
carbide	Processed	8.6	10,479,199	0.977
Graphite	Raw	1.4	16,082,511	0.994
fibres	Processed	1.4	20,103,139	0.994

a large amount of TCE material. The next step, however, yields smaller reduction in the plant cost but results in the same increase in TCE cost. At some point, based on the price of each thermal conductivity improvement step, the cost reduction of the plant is no longer larger than the cost of the additional TCE material. For example, Fig. 6 shows the cost reduction optimum for aluminium to be somewhere about five to six times the average PCM thermal conductivity.

This optimal level of thermal conductivity enhancement is different for each material based on the thermal conductivity and the price. Table 8 shows the result of this analysis for each material. The pool of materials has been greatly reduced to only the materials that show LCOE reduction.

These materials are then plotted as function of TCE level on the break-even function to give some idea of the best material available and the best level of TCE. Fig. 7 shows the materials of interest with the
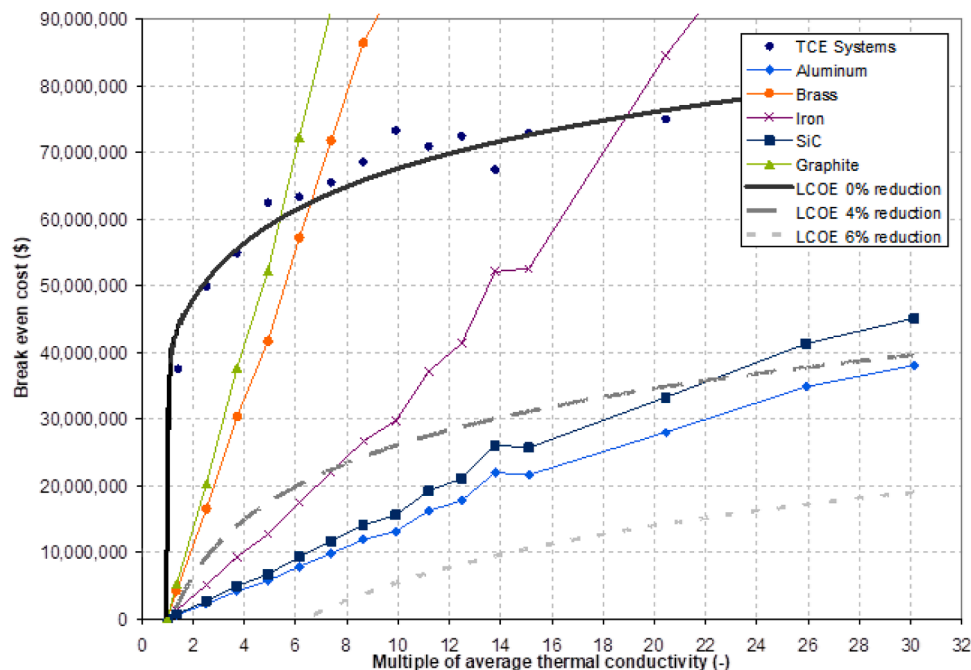

Fig. 7. TCE materials of interest with error bars representing unknown processing cost.

Table 9
Maximum void fractions achievable by naturally shaped objects [25].

Material	Sphericity	Natural void fraction
Ottawa sand	0.95	0.42
Rounded sand	0.83	0.44
Coal dust	0.73	0.46
Flint sand	0.65	0.48
Crushed Glass	0.65	0.48
Mica flakes	0.28	0.63

break-even curve. Additionally, it shows the break-even curves for systems with 4% and 6% LCOE reduction. Based on this plot aluminium has been chosen as the best TCE material. This is based on not only the possibility of it giving us the lowest cost system but also on its low processing and cost uncertainty.

To reach the ideal thermal conductivity multipliers seen in Fig. 7, high void fractions are required: 0.919 for aluminium. However, as discussed, high processing costs cannot be tolerated. This means that highly engineered products like foams are not an appropriate way to reach the required void fractions.

An obvious choice to reduce processing cost is to use a natural packing approach. Here, minimal processing would be used to grind or cut the TCE before submersion into the PCM. Natural packing is used in a thermocline to achieve necessary void fractions because the sand and gravel filler is unprocessed. It is necessary to test if the proper void

fraction for our system can be achieved with natural packing. Based on correlations derived by Wen and Yu, the void fraction of a system using natural packing can be calculated using a sphericity equation, Eq. (2) [26]:

$$\Phi = \frac{1}{14\alpha^3} \tag{2}$$

where: Φ = sphericity
α = void fraction

This equation is based on the sphericity of the object being packed. Natural objects have a sphericity defined by the similarity between their shape and a perfect sphere; objects like stones tend to have a high level of sphericity where objects with flake-like structures tend to have the lowest level of sphericity in nature, somewhere near 0.2. Table 9 lists the void fractions that can be achieved using naturally shaped objects. Fig. 8 also shows the maximum achievable void fraction with naturally packing object in addition to the void fraction required for our system.

Clearly, natural packing will not meet the required void fraction criteria. This reintroduces the need for material processing. As discussed previously, materials that need significant processing, machining, casting, forging, or foaming, will not be cost competitive for the application. Therefore, packing materials that have an inherent engineered structure should be found.

Aluminium is a heavily recycled material. As such, it may be possible to acquire pre-processed recycled aluminium that still has a highly
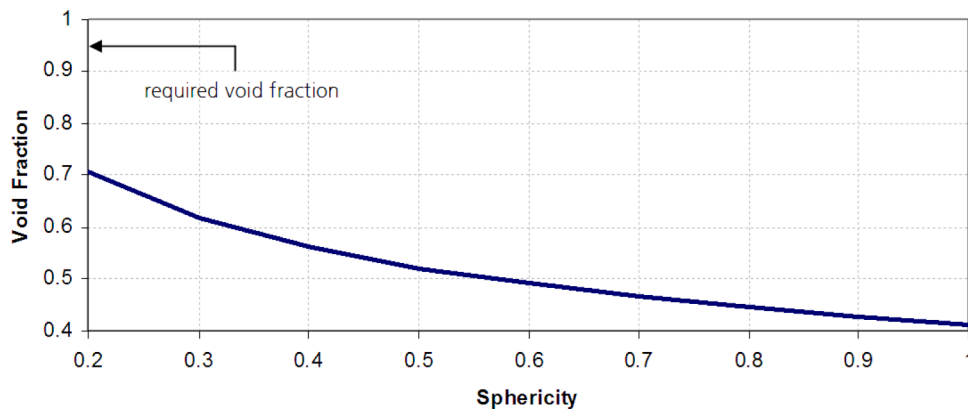

Fig. 8. Void fraction achievable by naturally packing shapes with given sphericity.
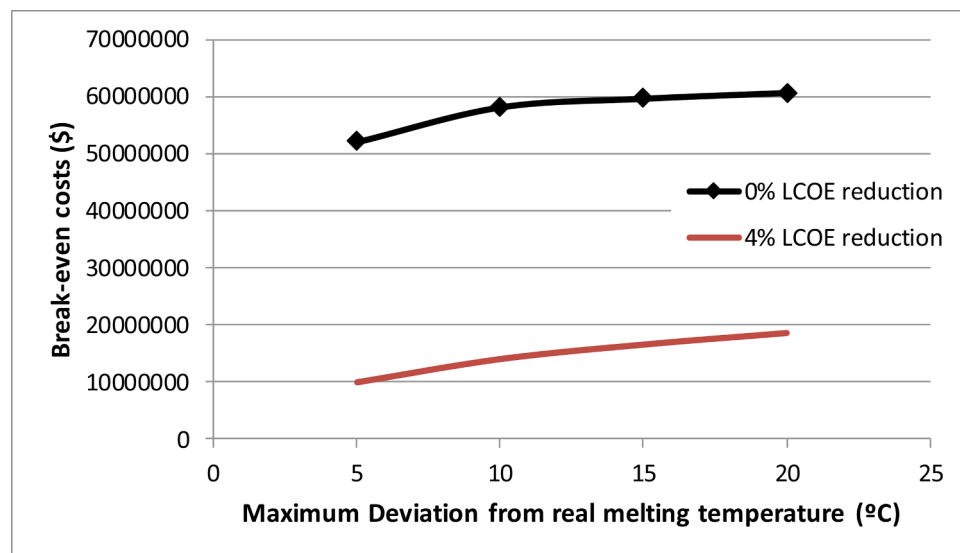

Fig. 9. Breakeven function for different amounts of melting temperature modification.

Table 10

System dimensions for the TCE storage system.

Dimension	Value	Unit
Tube diameter	0.02	m
Tube length	250	m
PCM radial extent bucket 1	3.75	cm
PCM radial extent bucket 2	4.00	cm
PCM radial extent bucket 3	3.25	cm
PCM radial extent bucket 4	3.25	cm
Number of tubes in bucket 1	2100	-
Number of tubes in bucket 2	3600	-
Number of tubes in bucket 3	3600	-
Number of tubes in bucket 4	2652	-
T melt bucket 1	320	°C
T melt bucket 2	340	°C
T melt bucket 3	360	°C
T melt bucket 4	380	°C

Table 11

System dimensions for the ideal thermal properties PCM storage case.

Dimension	Value	Unit
Tube Diameter	0.02	m
Tube Length	250	m
PCM radial extent bucket 1	3.75	cm
PCM radial extent bucket 2	4.00	cm
PCM radial extent bucket 3	3.25	cm
PCM radial extent bucket 4	3.25	cm
Number of tubes in bucket 1	2500	-
Number of tubes in bucket 2	4000	-
Number of tubes in bucket 3	4000	-
Number of tubes in bucket 4	2500	-
T melt bucket 1	320	°C
T melt bucket 2	340	°C
T melt bucket 3	360	°C
T melt bucket 4	380	°C
Thermal properties based on	MgCl2-KCl-NaCl	-

engineered structure from its previous life. An example of this concept would be recycled aluminium tubes. Aluminium tubes are prolific in recycling bound waste streams in the form of used structure beams, containers, and building materials. Furthermore, these tube structures

can readily achieve the void fractions required by the system. For example, if aluminium tubes with the dimensions of common soda cans were to be dumped into our PCM storage tanks, they would naturally reach a void fraction of 0.98.

4.2. Influence of the melting temperature of the PCM

The effect of well-spaced PCMs was investigated as a solution to unstable operation caused by the dissimilar pinch points during charge and discharge. Instead of finding completely new PCMs slight modifications in melting point can be accomplished through doping with other salts. Currently, two national labs and several private entities are working of either the development of novel PCMs or the alteration of current PCMs.

To find the most appropriate set of melting temperatures a tolerance on melting points was successively relaxed from 0 °C to 20 °C. When the tolerance was relaxed, the melting points were allowed, but not forced, to move as far as the new tolerance.

Fig. 9 shows the breakeven function generated by the movement of this melting temperature modification tolerance from 0 °C to 20 °C. Similar to the TCE breakeven plot, there is a point of diminishing returns where, even though the tolerance is relaxed further, meaningful cost savings are not realized.

Using this plot, a melting temperature movement tolerance of 10 °C was chosen and a parametric study was used to generate an acceptable set of system dimensions. These dimensions are summarized in Table 10.

4.3. Ideal properties PCM

In addition to more appropriate melting points, the effect of more appropriate thermal properties was also investigated. If the enthalpies of fusion, thermal conductivities, specific heats, or densities of the PCMs currently being used are improved, the performance of the system can be improved. In order to keep the investigation grounded in reality, the PCM with the best thermal properties, $MgCl_2$-KCl-NaCl, was used to set the thermal properties for all the PCMs.

Once the thermal properties were assigned, a new system was parametrically derived with acceptable performance. Table 11 shows
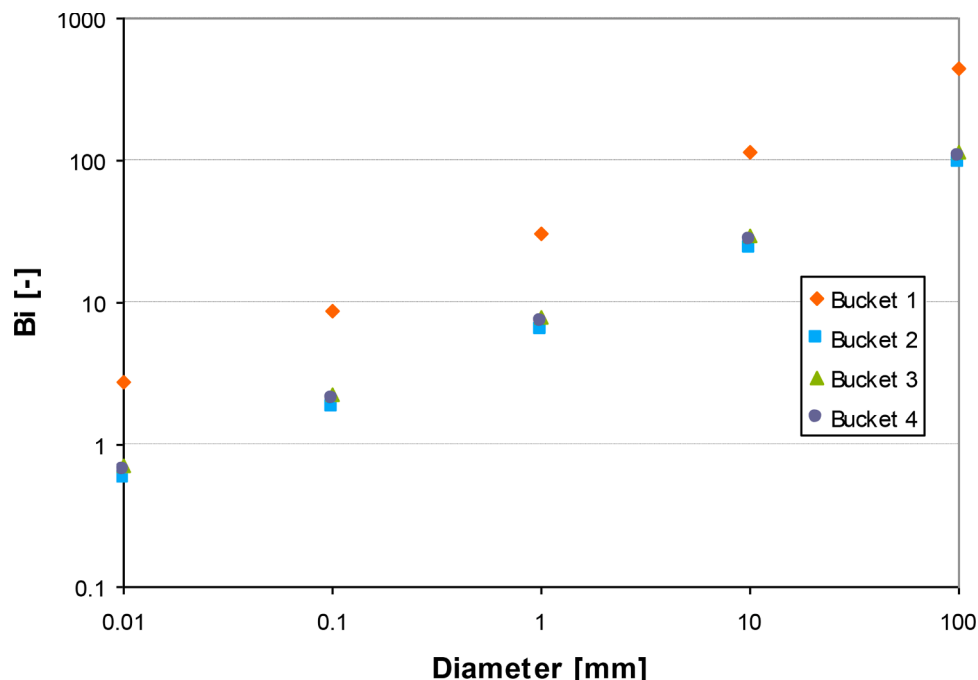

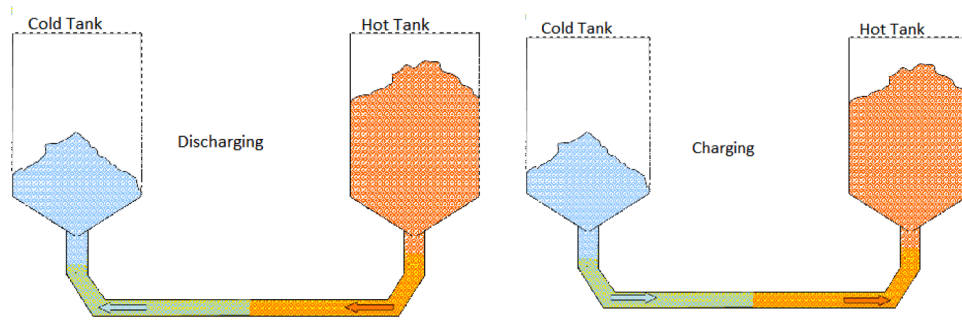**Fig. 10.** Biot number for various size capsules.

Fig. 11. Discharging and charging flow regimes for a two tank encapsulated PCM system.

the system dimensions that were used.

4.4. Encapsulated PCM system

Encapsulation was proposed in phase one of this study as a method to improve the performance and reduce the cost of a phase change material thermal energy storage system. The basic PCM system proposed previously, a shell and tube heat exchanger with stationary PCM shell-side, suffers from high capital expense of the heat exchanger and low conductivity of the relatively large volume of PCM. Encapsulation can alleviate these problems by replacing the heat exchanger with cheaper tanks and increasing the surface area for heat transfer. In the study, the capsules had to be a manufacturable size. Second, the size was limited by the melting time. The Biot number was calculated to determine whether internal heat transfer would inhibit the uniform melting of the capsules. Third, the void fraction of the capsules was limited by the geometries of packed beds and slurries.

Fig. 10 shows the Biot number as a function of capsule diameter over a reasonable range. In each system, the Biot number and melt time were balanced against other parameters, specific to each system, to find a reasonable operation level. In the packed beds, pressure losses and the containment system limited the capsules minimum diameter. In the secondary fluid heat exchanger and pumped slurry systems, manufacturability was the main minimum size constraint

In tandem with the other physical modifications that were investigated, an encapsulated PCM system (Fig. 11), similar to a slurry, was also modelled. This system is a direct evolution of the shell and tube system: due to the encapsulation, the tube registry is no longer needed.

Furthermore, since the PCM is in direct contact with the HTF, it is more appropriate to pump the PCM between two solid storage tanks instead of purchasing large pressure vessels to hold all the PCM submerged in HTF.

The pumped slurry (Fig. 12) is similar to the baseline two tank system. Pairs of tanks are filled with 35% encapsulated PCM by volume and the remainder is filled with molten salt. All four PCMs are distributed in the slurry with their mass ratios scaled to each store an equal amount of energy. The slurry is pumped through a heat exchanger like that in the two-tank baseline system.

Although this system is physically very similar to the PCM system, its performance is closer to a two-tanks system, so the performance of the encapsulated system was assumed to be the same as the two tanks baseline case. The direct packed bed system will likely require excessive storage vessel costs because the entire system must be maintained at 10 bars, the vapor pressure of Therminol. The performance should be similar to that of the basic PCM system because the control scheme is very similar. This system suffers from poor performance in partial charge/discharge. Before modelling, it is unclear whether the cost of encapsulation, heat exchanger, and storage tanks in an indirect packed bed will outweigh the benefit of eliminating the cost of the shell and tube heat exchanger.

The cost of the system was generated using some basic assumptions. These were:

1. Solid storage tank costs were scaled from the tank costs of the baseline storage tanks by the mass of carbon steel needed to store the solids.
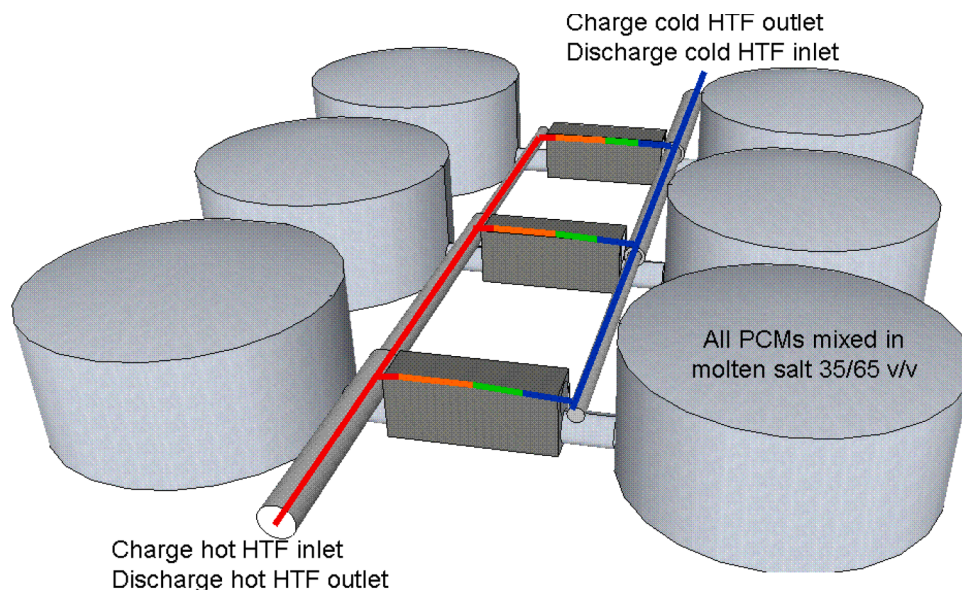

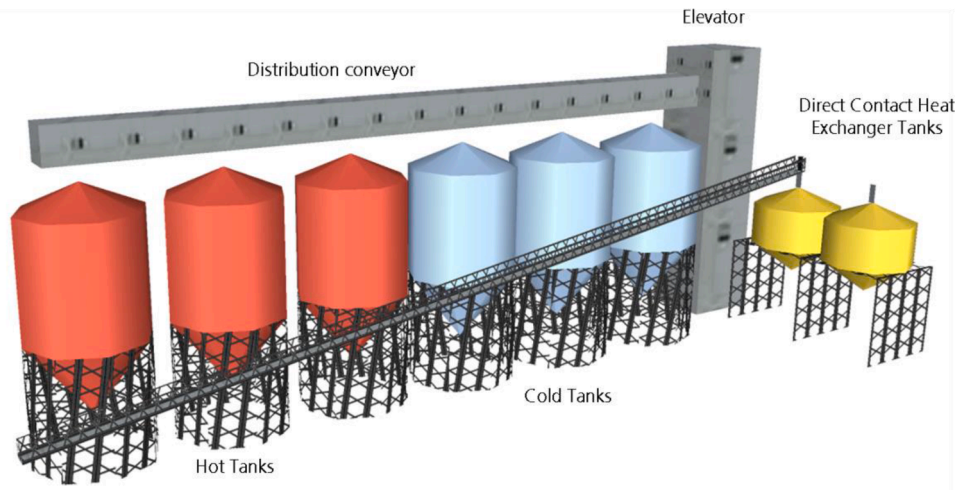**Fig. 12.** Generalized pumped slurry design.

Fig. 13. Current design of a single bucket in the encapsulated PCM system.
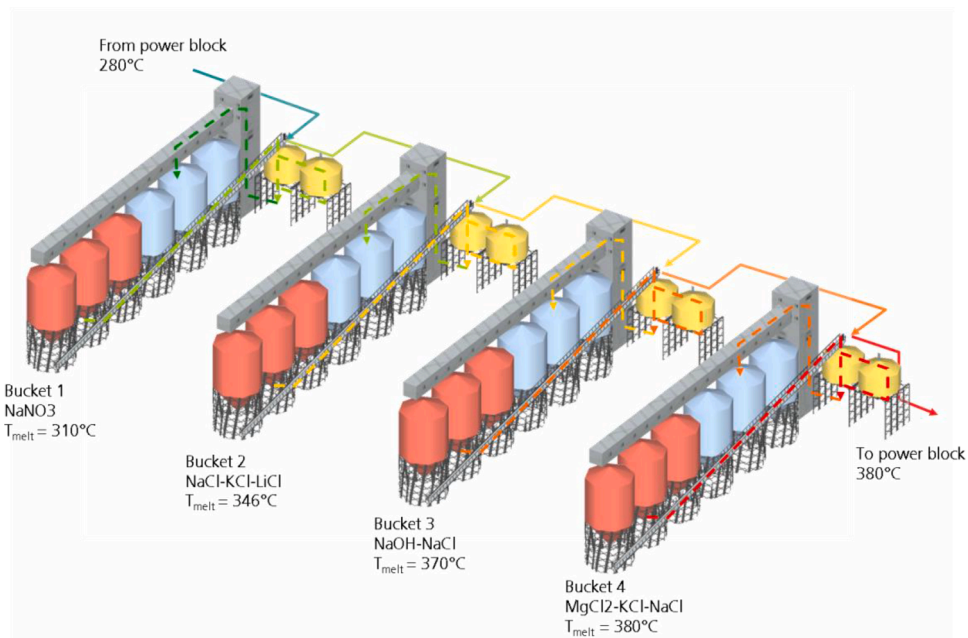

Fig. 14. Discharge flow paths of the HTF and PCM in an encapsulated system.

2. The thickness of the baseline storage tanks is assumed for the solid storage tanks.
3. The insulation cost was calculated on an area basis from the EPC baseline quote.
4. The foundations cost was calculated on an area basis from the EPC baseline quote.
5. The pump cost was calculated assuming a 2 bar pressure drop in the HTF.
6. Elevator and conveyor equipment similar to a grain elevator is assumed for the cost of the PCM movement system.

Although the system is conceptually a short extension of the shell and tube PCM system, the actual system layout looks significantly different. To assume that the operation is drastically different is incorrect. The difference in physical layout stems from the solid nature of the PCM. Because the PCM now has its own heat exchanger surface, the encapsulation shell, it is more cost effective to use a direct contact heat exchanger to transfer the energy to and from the PCM. Once this is implemented it is more cost effective to store the PCM in solid storage

tanks and use conveyor systems to more it to and from the direct contact heat exchanger. It is this solid distribution system that drastically alters the look of the storage system. However, conceptually it is just a simple evolution of the shell and tube system. Instead of metal tubes, an encapsulating micro layer is used to separate the HTF from the PCM and instead of the PCM sitting in a heat exchanger it is pumped against the HTF. These two simple evolutions on the system may drastically reduce both the cost, and the transient nature of the PCM. Fig. 13 shows the system as currently envisioned.

When considering the entire system, the charge/discharge motion of the HTF is almost identical to the shell and tube system. However, now there is also a movement to the PCM. This new charge/discharge flow paths are shown in Figs. 14 and 15.

4.5. Compact heat exchanger

As an alternative to shell and tube heat exchangers, compact heat exchangers were also analysed as a method of reducing the tube registry cost. In theory, compact heat exchangers have better overall heat
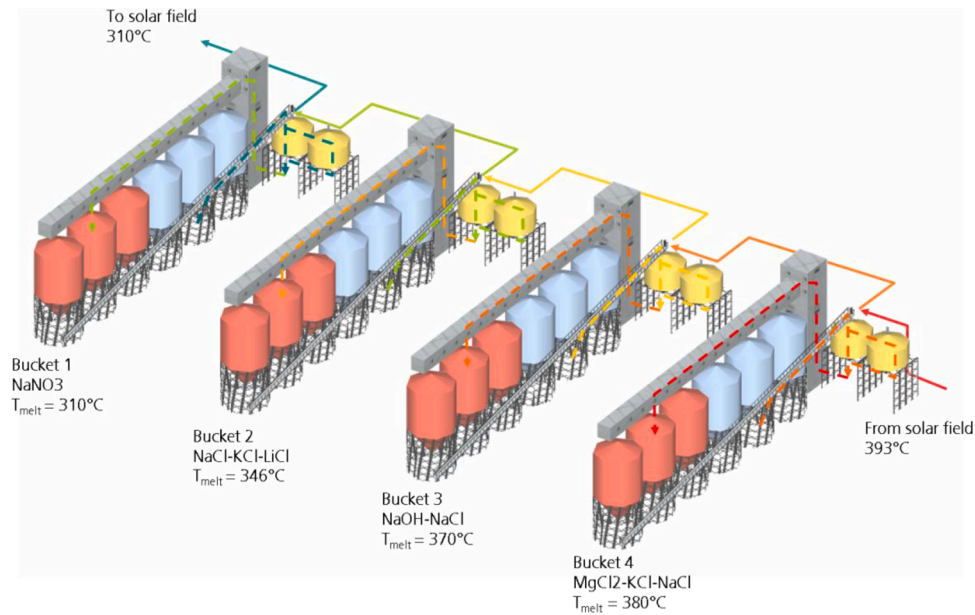
Fig. 15. Charging flow paths of the HTF and PCM in an encapsulated system.
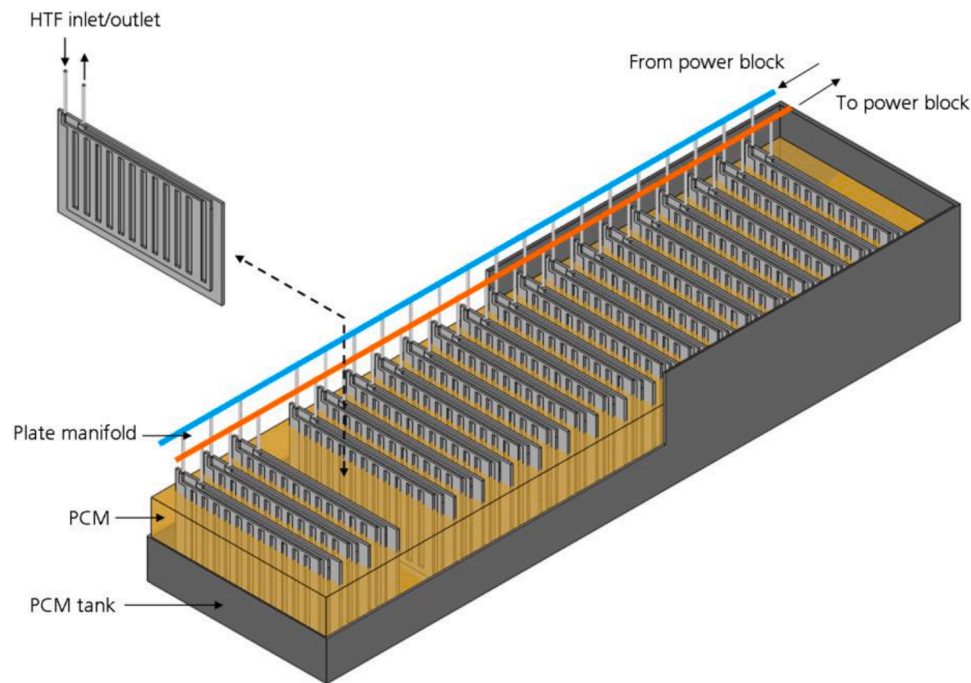

Fig. 16. Conceptual schematic of an expanded plate system.

transfer then shell and tube heat exchangers. As such, they may represent an avenue toward reduction of the system cost.

There are several types of compact heat exchangers that were initially considered: plate and frame, plate and tube, fin and tube, and expanded plate. Most of these heat exchangers have a severe drawback; the PCM side is constrained volumetrically to be near that of the HTF side. This leads to systems with high heat exchanger costs just to store the PCM. As such, the expanded plate type heat exchanger was selected as the best candidate (Fig. 16).

4.6. Enhanced thermal properties

In addition to each individual PCM variation, some examples of

superposition were also investigated. This variation, known as Enhanced thermal properties, combines the thermal conductivity enhancement, and ideal thermal properties.

The system configuration was determined by using the ideal properties, melting point, and level of TCE for each individual variation. Although a new set of melting points, or level of TCE, might be more appropriate for the mixed system, the same values were used. By doing this, the effect of variation combination was tested. Theoretically, the different improvements should combine in a fairly linear manner. In reality this was not observed. The resulting system offers the lowest cost system investigated, however, the reduction in cost does not represent a direct superposition of each individual improvement.

Table 12
Cost breakdown of the considered scenarios ($).

|	Baseline	Encapsulated PCM	Basic PCM	Compact Heat Exchanger Design	Ideal Temperature PCM	Ideal Properties PCM	Enhanced Ideal Properties	TCE PCM
Heat Exchanger	23,480,029	24,619,114	52,764,613	96,617,949	46,768,629	46,396,796	16,801,838	20,140,207
Storage Material	69,303,348	69,106,478	31,923,734	24,086,610	28,662,411	11,265,649	10,716,144	26,720,236
HTF	0	0	5,699,295	9,077,890	5,052,350	5,009,245	1,825,437	2,185,590
TCE	0	0	0	0	0	0	4,271,563	4,640,591
Other	33,252,464	22,989,390	17,013,723	1,062,809	15,241,399	13,722,265	12,456,319	13,215,886
Tanks	35,643,851	18,233,125	0	0	0	0	0	0
TES pumps	2,548,638	0	0	0	0	0	0	0
Salt Melting	15,473,459	0	12,983,968	12,983,968	12,983,968	12,983,968	12,983,968	12,983,968
TES cost	181,208,060	134,948,107	120,385,333	143,829,227	108,708,757	89,377,923	59,055,270	79,886,479
Plant cost	938,923,067	906,456,099	880,857,556	891,909,174	869,067,682	849,729,299	818,849,066	839,743,349
Uncertainty	24,077,067	26,989,621	24,077,067	28,765,845	21,741,751	17,875,585	11,811,054	15,977,296
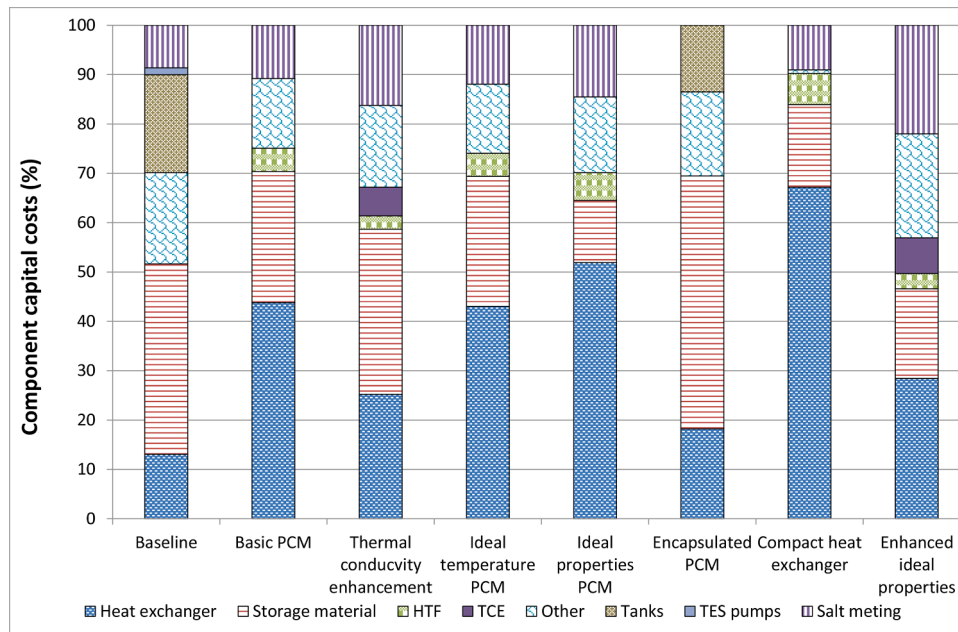
Fig. 17. Cost breakdown of the considered scenarios.

5. Results

Using the EPC quote and cost functions, the capital cost for the Baseline, Basic PCM, and all PCM variations were generated. Specifications not impacted by the switch to PCM TES (e.g., fences, building. etc.) were maintained from the baseline plant. The estimates included extreme detail ranging from large items such as the turbine down to minor items such as safety showers, fences, and buildings. The final estimates totalled 420+ pages of itemized materials for each plant. While the thoroughness of these estimates and past experience of EPC point to a reduced uncertainty, the lack of detailed engineering drawings required EPC to specify an uncertainty of ±20% based on accepted estimating practices. Table 12 shows capital cost breakdowns calculated for all system considered. The total TES system costs are generally lower for the PCM systems. Fig. 17 shows the total cost of the TES system with broken down constituent costs and cost uncertainties.

Although in general the PCMs have lower costs. It is also important to note that the performance of the systems is different. The annual net output is slightly lower for the PCM case. As such, the performance must be taken into account by using levelized cost metrics whenever the two systems are compared. The first metric used in this analysis is the cost performance quotient (CPQ). This metric represents the cost of each kWh net electric generated from the storage system and is calculated

with:

$$CPQ = \frac{Cost_{TES}}{E_{storage,net}} \tag{3}$$

Although LCOE is also used to compare the storage system, CPQ is a better comparison method because it does not have a cost ceiling. Because the TES system is only 10-20% of the total capital cost of a plant, the reduction of the TES cost to zero only results in 10-20% reduction in LCOE. This means that any real technological based cost reduction, even if it is ground breaking, is likely to reduce the LCOE less than 10%. Fig. 18 show the CPQ and reductions from the baseline for each of the PCM variant.

Although the LCOE has a cost reduction ceiling limiting its effectiveness as a comparison metric, it is still the most complete method of comparison. This is because it takes all the costs, O&M, and financing into account when it is calculated. Although the LCOE is the most complete way of comparing the different technologies considered, it is not appropriate to compare the LCOE values calculated here to other published LCOE values. This is because the economic model used for our analysis is likely to be different than any other analysis. Fig. 19 give the LCOE values, reductions, and uncertainties for the baseline and all the PCM variants.

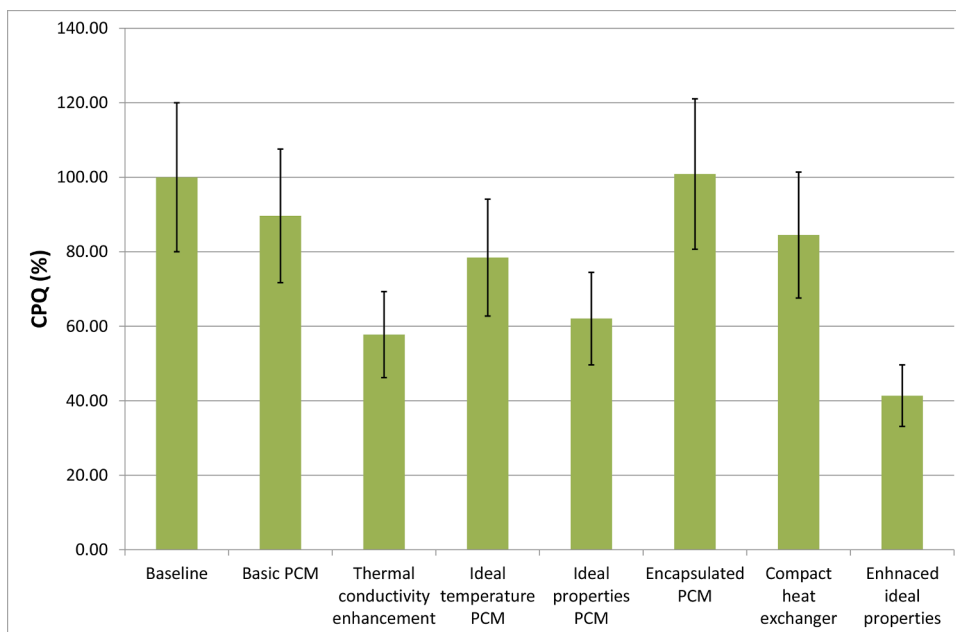Fig. 19 shows that all considered scenarios have an LCOE between

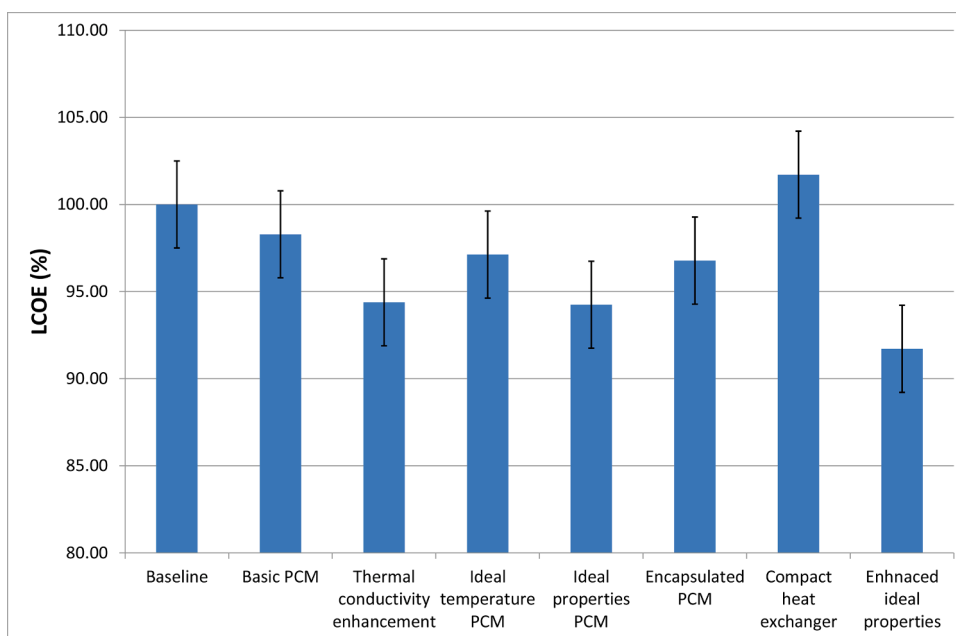**Fig. 18.** CPQ reduction for the considered scenarios.

Fig. 19. LCOE values and reduction for the considered scenarios.

92% and 102% of that of the baseline. The option with highest LCOE reduction is the use of materials with enhanced properties, closely followed by the thermal conductivity enhancement and the use of PCMs with ideal properties. Since finding a PCM with the ideal properties is quite difficult, the option with closest potential to implementation is the thermal conductivity enhancement.

6. Conclusions

PCM TES has been shown to have lower levelized costs than the baseline two tanks system. This has been shown to be true for both the LCOE and the CPQ. Shell and tube PCM storage offers a reduction in capital and levelized cost. Furthermore, there exist several avenues for further cost reduction. These PCM variants have been studied to the

point where some confident exists in their merit. However, more research is required to determine the best avenue forward.

In addition to these conclusions, it has also been shown that transient storage systems like PCM need annual, modelling, discretised to at least the hourly level, of many charge-discharge cycles to fully be understood. A simple charging or discharging model is insufficient to capture the complex transient coupled interactions between the plant and storage system.

Additionally, it has been shown that a control strategy or sizing paradigm focused solely on maximizing performance is not acceptable. It has been shown that a control strategy with a focus on day-to-day repeatability and system stability is critical to the full utilization and lasting performance of the system.

Although the basic shell and tube PCM system has been shown to

offer a cost savings, the 1.8% reduction in LCOE may not be worth the risk of further development. The shell and tube system should be a jumping off point to more appropriate technologies. These technologies might include thermal conductivity enhancement, PCM encapsulation, PCM modification, a combination of these, or a completely new variant. Together these technologies are likely to yield cost reductions in CPQ as high at 80% and in LCOE as high as 10%. This represents a drastic, unprecedented, and valuable avenue of CSP plant cost reduction.

CRediT authorship contribution statement

Cristina Prieto: Conceptualization, Methodology, Software, Validation, Investigation, Resources, Writing – review & editing, Supervision, Project administration, Funding acquisition. **Luisa F. Cabeza:** Conceptualization, Methodology, Formal analysis, Resources, Data curation, Writing – original draft, Visualization, Supervision, Project administration, Funding acquisition.

Declaration of Competing Interest

The authors declare that they have no known competing financial interests or personal relationships that could have appeared to influence the work reported in this paper.

Acknowledgements

References

[1] E. González-Roubaud, D. Pérez-Osorio, C. Prieto, Review of commercial thermal energy storage in concentrated solar power plants: Steam vs. molten salts, Renew. Sustain. Energy Rev. 80 (2017) 133–148, https://doi.org/10.1016/j.rser.2017.05.084.

[2] X. Zhuang, X. Xu, W. Liu, W. Xu, LCOE analysis of tower concentrating solar power plants using different molten-salts for thermal energy storage in China, Energies 12 (2019) 1394, https://doi.org/10.3390/en12071394.

[3] C. Parrado, A. Marzo, E. Fuentealba, A.G. Fernández, 2050 LCOE improvement using new molten salts for thermal energy storage in CSP plants, Renew. Sustain. Energy Rev. 57 (2016) 505–514, https://doi.org/10.1016/j.rser.2015.12.148.

[4] K. Gawlik, Reducing the Cost of Thermal Energy Storage for Parabolic Trough Solar Power Plants, Golden, CO (United States), 2013. doi:10.2172/1090094.

[5] NREL, Concentrating Solar Power Projects with Operational Plants, (2020).

[6] A. Palacios, C. Barreneche, M.E. Navarro, Y. Ding, Thermal energy storage technologies for concentrated solar power – A review from a materials perspective, Renew. Energy 156 (2020) 1244–1265, https://doi.org/10.1016/j.renene.2019.10.127.

[7] O. Achkari, A. El Fadar, Latest developments on TES and CSP technologies – Energy and environmental issues, applications and research trends, Appl. Therm. Eng. 167 (2020), 114806, https://doi.org/10.1016/j.applthermaleng.2019.114806.

[8] M. Mofijur, T. Mahlia, A. Silitonga, H. Ong, M. Silakhori, M. Hasan, N. Putra, S. M. Rahman, Phase Change Materials (PCM) for solar energy usages and storage: an overview, Energies 12 (2019) 3167, https://doi.org/10.3390/en12163167.

[9] R. Muren, D.A. Arias, B. Luptowski, Performance based cost modeling of phase change thermal energy storage for high temperature concentrating solar power systems, in: ASME 2009 Int. Mech. Eng. Congr. Expo., ASME, Lake Buena Vista, Florida, USA, 2009, pp. 193–202, https://doi.org/10.1115/IMECE2009-12848.

[10] R. Tamme, D. Laing, W.-D. Steinmann, Advanced thermal energy storage technology for parabolic trough, in: ASME 2003 Int. Sol. Energy Conf., ASME, Kohala Coast, Hawaii, USA, 2003, pp. 563–571, https://doi.org/10.1115/ISEC2003-44033.

[11] H. Michels, R. Pitz-Paal, Cascaded latent heat storage for parabolic trough solar power plants, Sol. Energy. 81 (2007) 829–837, https://doi.org/10.1016/j.solener.2006.09.008.

[12] Luz International, Phase-change thermal energy storage: Final subcontract report, Golden, CO, 1989. doi:10.2172/5159078.

[13] B. Zhao, M. Cheng, C. Liu, Z. Dai, Thermal performance and cost analysis of a multi-layered solid-PCM thermocline thermal energy storage for CSP tower plants, Appl. Energy. 178 (2016) 784–799, https://doi.org/10.1016/j.apenergy.2016.06.034.

[14] G. Cáceres, M. Montané, S. Nasirov, R. O'Ryan, Review of thermal materials for CSP plants and lcoe evaluation for performance improvement using chilean strategic minerals: Lithium salts and copper foams, Sustain 8 (2016), https://doi.org/10.3390/su8020106.

[15] R. Jacob, M. Belusko, A. Inés Fernández, L.F. Cabeza, W. Saman, F. Bruno, Embodied energy and cost of high temperature thermal energy storage systems for use with concentrated solar power plants, Appl. Energy 180 (2016) 586–597, https://doi.org/10.1016/j.apenergy.2016.08.027.

[16] C. Prieto, L.F. Cabeza, Thermal energy storage (TES) with phase change materials (PCM) in solar power plants (CSP). Concept and plant performance, Appl. Energy 254 (2019), 113646, https://doi.org/10.1016/j.apenergy.2019.113646.

[17] A. Gil, M. Medrano, I. Martorell, A. Lazaro, P. Dolado, B. Zalba, L.F. Cabeza, State of the art on high temperature thermal energy storage for power generation. Part 1 — Concepts, materials and modellization, Renew. Sustain. Energy Rev. 14 (2010) 31–55, https://doi.org/10.1016/j.rser.2009.07.035.

[18] G.J. Janz, C.B. Allen, N.P. Bansal, R.M. Murphy, R.P.T. Tomkins, Physical properties data compilations relevant to energy storage. II. Molten salts: data on single and multi-component salt systems, (1978).

[19] C. Prieto, R. Osuna, A.I. Fernández, L.F. Cabeza, Thermal storage in a MW Scale. Molten salt solar thermal pilot facility: plant description and commissioning experiences, Renew. Energy (2016), https://doi.org/10.1016/j.renene.2016.07.053.

[20] O. Mesalhy, K. Lafdi, A. Elgafy, K. Bowman, Numerical study for enhancing the thermal conductivity of phase change material (PCM) storage using high thermal conductivity porous matrix, Energy Convers. Manag. 46 (2005) 847–867, https://doi.org/10.1016/j.enconman.2004.06.010.

[21] Metal prices, (2020). https://www.metalary.com/aluminum-price/.

[22] Silicon carbide price, (2020). www.bandbrefractory.com/silcon-carbide-scrap.html.

[23] Carbon fibres price, (2020). www.recycle.net/Minerals/carbon/xv080300.html.

[24] Beryllium price, (2020). www.ibcadvancedalloys.com/s/AboutBeryllium.asp.

[25] Discussion with Thomas Golubic; local sales rep; Koppers carbon foam supplier, (2020).

[26] C.Y. Wen, Y.H. Yu, Mechanics of fluidization, Chem. Eng. Prog. Symp. Ser. 162 (1966) 100–111.